Pakistan Veterinary Journal

ISSN: 0253-8318 (PRINT), 2074-7764 (ONLINE)
DOI: 10.29261/pakvetj/2020.012

RESEARCH ARTICLE

Expression of Canine Kynurenine 3-Monooxygenase by Baculovirus for Canine Mammary Tumor Diagnosis

Hui-Yu Chen[1], Cheng-Chi Liu[1], Bang-Hung Liu[1] and Chen-Si Lin[1, 2]*

[1]Department of Veterinary Medicine, National Taiwan University, Taipei, Taiwan
[2]Animal Cancer Center, College of Bioresources and Agriculture, National Taiwan University, Taipei, Taiwan
*Corresponding author: cslin100@ntu.edu.tw

ARTICLE HISTORY (19-319)

Received: July 28, 2019
Revised: January 05, 2020
Accepted: January 09, 2020
Published online: February 03, 2020

Key words:
Baculovirus expression system
Canine cancer diagnosis
Carcinogenesis
Kynurenine 3-monooxygenase
Kynurenine pathway

ABSTRACT

Kynurenine 3-monooxygenase (KMO), an outer mitochondrial membrane enzyme that is central to the kynurenine pathway, has been demonstrated to be associated with malignancy in human cancers. Cancers in dogs are considered reliable and clinically relevant models of human diseases owing to similarities in the natural history of these human and canine tumors and the superficial resemblances in the anatomy, topology, metastatic patterns, and response to therapy between canine and human cancers. This study aims to establish an efficient protocol to prepare the recombinant canine KMO protein for potential application in canine cancer study. The amino acid sequence and structure of canine KMO were analyzed using homology modeling provided by SWISS-MODEL. The canine KMO (cKMO) was produced by using a baculovirus–insect cell (Sf9 cells) expression system. Full-length cKMO was expressed by the baculovirus-infected Sf9 cells as a 477-amino-acid protein with a molecular weight of 55 kDa. On average a yield of 2 mg of protein was obtained from 2×10^8 baculovirus-infected Sf9 cells. The results from western blot and immunofluorescent assay showed KMO can be successfully expressed by Sf9 cells within the cytosol and mitochondria. The purified recombinant KMO protein could be used as an antigen for generating anti-cKMO antibodies to further investigate the role in canine carcinogenesis.

To Cite This Article: Chen HY, Liu CC, Liu BH and Lin CS, 2020. Expression of canine kynurenine 3-monooxygenase by baculovirus for canine mammary tumor diagnosis. Pak Vet J, 40(2): 145-150. http://dx.doi.org/10.29261/pakvetj/2020.012

INTRODUCTION

Canine mammary tumors (CMTs) are among the most common tumors in female dogs, and half of these tumors are diagnosed as malignant. The prognosis of dogs with malignant CMTs is usually extremely poor (Moe, 2001; Merlo *et al.*, 2008). Surgery is the most commonly recommended and essential treatment for CMT removal, except in cases of inflammatory carcinomas (CS H, 2018). Therefore, developing effective diagnosis and treatment methods for CMTs is necessary.

Kynurenine-3-monooxygenase (KMO) is an enzyme involved in the tryptophan metabolic pathway and is mainly found on the outer mitochondrial membrane. Several metabolites from this pathway, such as quinolinic acid (QUIN) and kynurenic acid (KYNA), which are neurotoxic and neuroprotective, respectively, in the central nervous system, are reported to be associated with neurodegenerative diseases (Campbell *et al.*, 2014). However, in cancer pathogenesis, QUIN also has been reported to be involved in cell growth, while KYNA has been demonstrated to exhibit an antiproliferative property (Walczak *et al.*, 2012; Sahm *et al.*, 2013; Walczak *et al.*, 2014). These findings indicate that KMO plays a role in tumor development because KMO functions at the critical branching point that determines the synthesis of either QUIN or KYNA (Courtney, 2010).

Studies on cKMO and successful reports of extracellularly expressed cKMO are not currently available in the scientific literature. The expression of functionally active human KMO has been reported in mammalian cell (HEK293, COS-1) (Alberati-Giani *et al.*, 1997; Breton *et al.*, 2000). Human KMO has also been expressed in insect cells (Hi5) (Amaral *et al.*, 2013); however, the protein yield is low in both expression systems. The overall yield of recovered pure protein in mammalian cell was approximately 60-70%, which corresponds to 5 μg of pure enzyme per 10^6 cells. The

recombinant human KMO protein derived from insect cells yielded small quantities of the protein (0.5 mg L^{-1} of culture) with poor stability. Recently, expression of human KMO in *E.coli* was reported; the full-length KMO with a 6× His tag was predominantly expressed in the insoluble fraction, while the full-length KMO with 12× His and FLAG tags was mainly expressed in the soluble fraction. However, only 19% of enzyme activity was recovered during purification (Wilson *et al.,* 2014).

The inhibition of KMO has been widely investigated as a target for inhibiting neurodegenerative diseases (Smith *et al.,* 2016). However, the role of KMO in tumorigenesis has not been completely elucidated. There was one study showed that KMO was highly expressed in hepatocellular carcinoma (HCC) cells and was associated with a relatively short survival time in patients with HCC (Jin *et al.,* 2015). Our recent investigation firstly found canine KMO was overexpressed as a biomarker in canine mammary tumors and correlated with poor prognosis of CMT dogs. Furthermore, silencing KMO expression by siRNA decreased tumor cell viability to suggest KMO might play a role in tumor establishment (Chiu *et al.,* 2019).

Currently, the role of KMO in canine cancers has not been fully investigated, and the importance of developing a new diagnostic methods and therapeutic targets for CMTs is increasing because of the poor prognosis in dogs with CMTs and low effectiveness of currently available treatments. We expect that the successful expression of the recombinant protein cKMO might be further applied in the diagnosis and treatment of CMTs.

MATERIALS AND METHODS

Amino acid sequence analysis and prediction of cKMO: A complete 1.4 kb cKMO cDNA has been identified, sequenced and submitted previously in the NCBI GenBank (GenBank accession number: HQ154039). The predicted 477 amino acid sequence was multiple aligned with human, mice and swine KMO using DNAstar megalign clustal W method (version 4.2.4, DNASTAR Inc., USA). The characteristics of cKMO protein were also analyzed by DNAstar protean software. The online SWISS-MODEL workspace (http://swissmodel.expasy.org/workspace/) was employed to simulate a 3D structure of cKMO protein and SWISS Pdb Viewer (version 4.1.0) for visualization. On the basis of amino acid sequence alignment between the target protein and the template structure, this 3D structure was modeled along homology eukaryotic Saccharomyces cerevisiae KMO protein structure (Pdb id: 4J33.1).

Cell culture: The insect cell line Sf9 derived from *Spodoptera frugiperda* was cultured in a complete, serum-free and protein-free medium SF-900II SFM (Gibco, Thermofisher, MA, USA) supplemented with 1% antibiotics and incubated at 27°C in a nonhumidified incubator.

Transfection of Sf9 cells and amplification of baculoviral stock: Recombinant bacmid DNA was isolated using the Presto™ Midi Plasmid Kit (Geneaid, Taiwan). Approximately 8×10^5 Sf9 cells/well in a low-passage (5-20) state were seeded in a 6-well plate and were transfected with cKMO/bacmid by using the Cellfectin®II reagent (Invitrogen, MA, USA) according to the manufacturer's instructions available with the Bac-to-Bac® Baculovirus Expression system (Invitrogen, MA, USA). At 72 h after transfection, the first generation (P1) of viral stocks was produced. Then, the Sf9 cells were seeded at 2×10^6/well in a 6-well plate and infected with the P1 virus to generate high-titer P2 and P3 baculoviral stocks. The titer of recombinant the P3 baculovirus was measured through the endpoint dilution assay ($TCID_{50}$ assay) (O'Reilly *et al*., 1994). At 5 days after infection, the infected cells were examined through IFA by using anti-His antibodies.

Production of recombinant cKMO-baculovirus: A Bac-to-Bac kit® was used to prepare the recombinant cKMO-baculovirus. The cDNA sequence of cKMO (GenBank: HQ154039.1) was cloned into pFastBac™ HT A vector. The pUC/M13 primers specific to the flanking regions of the mini-attTn7 site of the bacmid were used to verify the transposition success with a PCR fragment of an expected size (Table 1).

Express of the recombinant cKMO protein: Sf9 cells were seeded at 2×10^6/well in a 6-well plate. The cells were infected with P3 viral stocks at multiplicities of infection (MOI) 1.5 and incubated at 27ºC for 72 hours. The expression of cKMO mRNA was determined through reverse transcription PCR (RT-PCR) from virus-infected Sf9 cells. The KMO438F/KMO962R primers for cKMO were used for amplification in PCR (Table 1). The PCR cycle parameters were as follows: pre-denaturation at 95ºC for 5 minutes, denaturation at 95ºC for 30 seconds, annealing at 60ºC for 40 minutes, followed by extension at 72ºC for 1 minutes. After 35 PCR cycles, a final extension step was maintained at 72ºC for 5 minutes. The expression of cKMO protein was confirmed using western blotting with the anti-His antibody (Proteintch, IL, USA). The insoluble protein from the virus-infected insect cells was extracted using 10% (w/v) IGEPAL® CA-630 and 5% (w/v) sodium deoxycholate (Sigma-Aldrich, Darmstadt, Germany) according to the method described by (O'Shaughnessy and Doyle, 2011).

Purification of recombinant cKMO protein through Ni-nitrilotriacetic acid agarose affinity chromatography: A 125 ml spinner flask with 50 ml of Sf9 cell culture was at a density of 2×10^6 cells mL^{-1}. The cells were infected with P3 viral stocks at MOI 1.5 and set the impeller stirring rate to 80-90 rpm at 27ºC. The cells were harvested when >50% of the infected cells were lysed. Approximately 2×10^8 cells were resuspended in 16 mL of denaturing lysis buffer (6 M Guanidine–HCl, 20 mM sodium phosphate, 500 mM NaCl, pH 7.8) and sonicated. The homogenized lysates were incubated overnight at room temperature with 2 mL of Ni-nitrilotriacetic acid agarose-filling column (Novagen, WI, USA) and equilibrated with a denaturing binding buffer (8 M Urea, 20 mM sodium phosphate, 500 mM NaCl, pH7.8). Subsequently, nonspecifically bound proteins were washed with 4 mL of wash buffer (8 M urea, 20 mM sodium phosphate, 500 mM NaCl, with or without 10 mM imidazole, pH6.8). Recombinant cKMO protein was

recovered with 5 mL of denaturing elution buffer (8 M urea, 20 mM sodium phosphate, 500 mM NaCl) supplemented with increasing concentrations of imidazole (0, 300, and 500 mM) and decreasing pH (pH 4 and 3). The fractions containing recombinant cKMO protein were concentrated using an Amicon Ultra-15 centrifugal filter device (Millipore, Darmstadt, Germany) with a molecular weight cutoff corresponding to 10,000 Da. The concentrated proteins in the buffer containing 8 M urea were then precipitated by adding nine volumes of ice-cold anhydrous ethanol for more than 1h incubation at -20°C, washed by 90% ice-cold ethanol, and resuspended in phosphate-buffered saline (PBS) with 0.1% sodium dodecyl sulfate (SDS). The BCA Protein Assay Reagent (Omicsbio, Taipei, Taiwan) was used to determine the concentration of proteins.

Subcellular location of recombinant cKMO in the Sf9 cells: The subcellular location of recombinant cKMO was examined through immunofluorescence analysis (IFA). In brief, 6 × 10^5 Sf9 cells were grown on coverslips and infected with P3 baculovirus in 12-well plate for 72 h. The cells were incubated for 15 min at 27°C in the presence of 100 nM MitoTracker® Red CMXRos (Invitrogen, MA, USA) and then fixed with 1 mL of 3.7% (v/v) paraformaldehyde in PBS at room temperature for 15 min. After washing twice, the cells were permeabilized using ice-cold acetone for 10 min at room temperature. The cells were then stained with a primary mouse anti-His (1:1000; GeneTex) monoclonal antibody followed by a fluorescein isothiocyanate (FITC)-conjugated anti-mouse secondary antibody (1:1000; MP Biomedical). The fluorescence indicated the location of KMO was visualized through fluorescence microscopy.

RESULTS

The analysis and prediction of KMO amino acid sequence and protein structure: The multiple alignments of the predicted 477 amino acid of cKMO with the other two species, human and mice were shown in Fig. 1A, where the sequence identity shared with canine is 84.3 and 81.1%, respectively. Three common sequence motifs of NAD(P)H-dependent flavin monooxygenase were highly conserved among these three species and highlighted with different color. These evidences supported the probability that cKMO belongs to NAD(P)H-dependent flavin monooxygenase. The predicted 3D structure showed that three conserved motifs of KMO among species locate at the middle and inner core (Fig. 1A). The structural characteristics of amino acid sequence were shown in Fig. 1C.

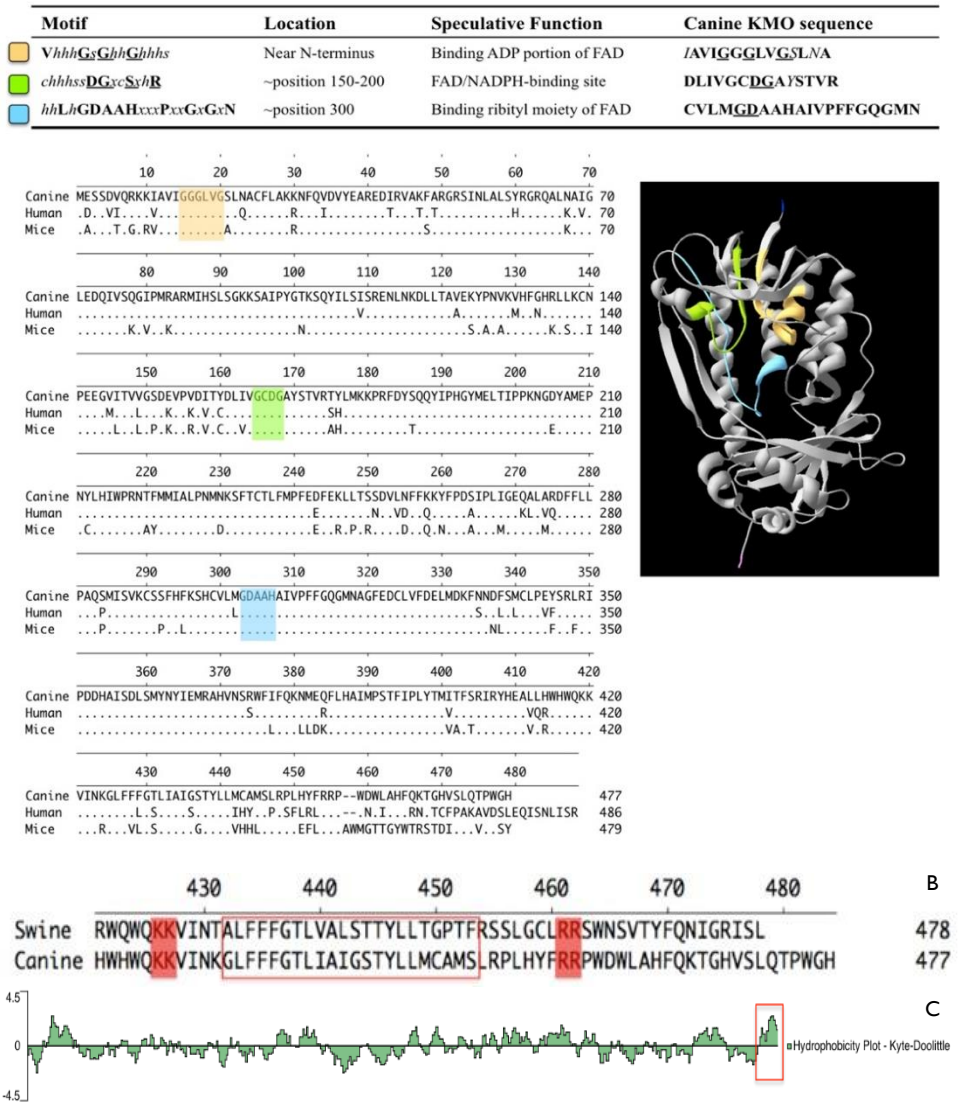

Fig. 1: Multiple amino acid sequence alignment from canine, human, mouse, and swine kynurenine-3-monooxygenase. (A) Three common sequence motifs of NAD(P)H-dependent flavin monooxygenase among the canine, human, and mouse forms are highlighted using different colors. The 3D structure of canine kynurenine-3-monooxygenase (KMO) (cKMO) was modeled using homology with the protein structure of *Saccharomyces cerevisiae* KMO by using SWISS-MODEL. The three conserved motifs corresponding to the different colors are listed in the upper panel. (B) The transmembrane domain of swine KMO is located in the residues 432–453 near the C-terminus and is flanked on both sides by basic amino acids, upstream (K426 and K417) and downstream (R461 and R462); cKMO exhibits the same pattern as swine KMO at the C-terminus. Deletion is marked with a dash (-), whereas identical regions are marked with a dot (·). (C)(NCBI reference sequence: *Homo sapiens*, NP_003670; *Mus Musculus*, NM_133809; *Sus. scrofa*, AAF80481).

Expressing canine KMO by baculovirus system: In this study, we reported for the first time the successful expression of recombinant cKMO protein with a full-length sequence and 6×His tag in a baculovirus–insect cell expression system and purification under denaturing conditions (Fig. 2). The results from this study indicated that a yield of 2 mg of purified recombinant cKMO protein was obtained from 2×10^8 Sf9 cells in 100 mL of culture. A relatively small quantity of protein was found in the soluble fraction when purified under native conditions (data not shown). However, the recombinant protein was predominantly expressed in the insoluble fraction.

Optimizing the expression conditions of canine KMO: Several variables were investigated while optimizing the expression condition to determine the expression kinetics of recombinant cKMO. Infection time is a critical factor affecting the maximum yield of recombinant protein because nonsecreted proteins are generally found to increase between 48 and 96 h after infection. Consistent with this expected trend, the Sf9 cells infected with P3 cKMO-baculovirus did not show any protein signal on Western blot analysis at 24 h after infection. Increasing the volume of baculovirus virus resulted in a stronger protein signal until 48 h after infection, which suggested that the expressed protein might have been partially degraded by intracellular protease released during Sf9 cells lysis. The optimal condition for expressing recombinant cKMO in this study was found in the lysates from cells infected 72-96 h with 200 µL P3 cKMO-baculovirus that corresponded to MOI of 1.5 after virus tittering and calculation (Fig. 3).

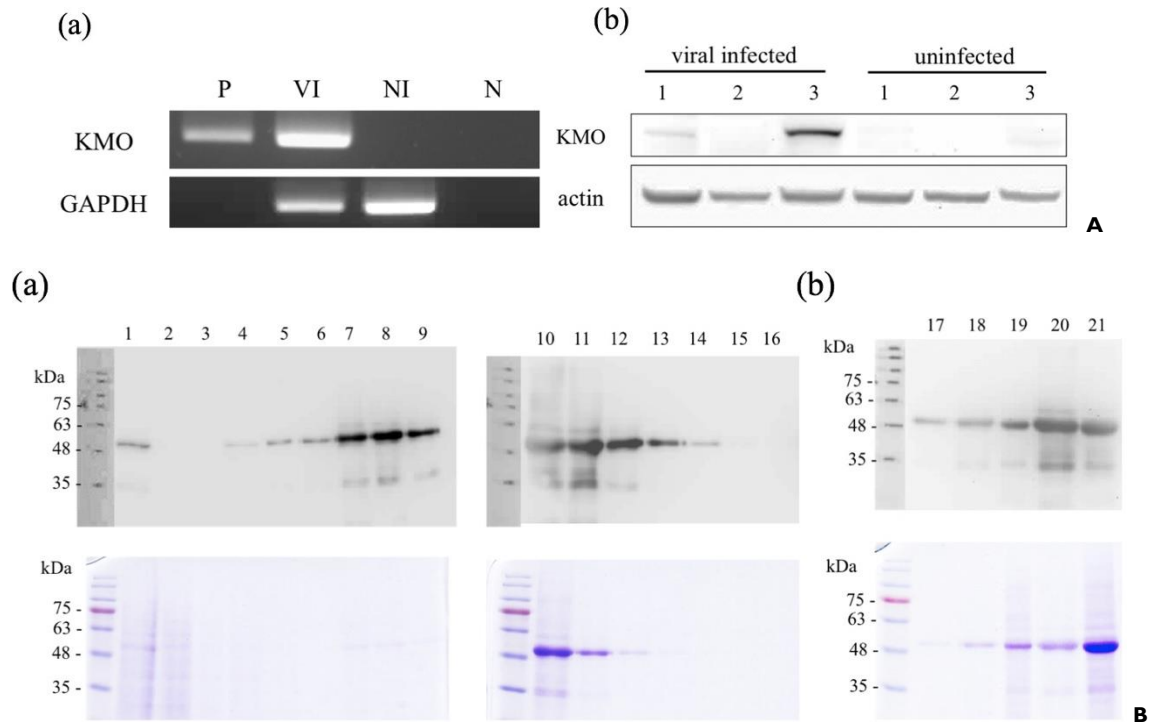

Fig. 2: Expression and denaturing purification of recombinant cKMO proteins in Sf9 cells. (A) mRNA and protein expression of recombinant cKMO in the Sf9 cells. (a) RT-PCR results showing mRNA expression of *cKMO* in the Sf9 cells. P, positive control; VI, virus-infected group; NI, non-infected group; and N, negative control. (b) Western blotting analysis confirmed the expression of recombinant His-cKMO protein by using anti-His as the primary antibodies. Lanes 1–3, different detergents: 1, lysis buffer; 2, IGEPAL® CA-630; 3, sodium deoxycholate. (B) Purification of recombinant cKMO protein under denaturing conditions. SDS-PAGE gel was stained using Coomassie brilliant blue, and Western blotting of His-cKMO (approximately 55 kDa) was conducted using anti-His as primary antibodies. (a) The purification fractions of purified protein are as follows: Lane 1, lysate (6 M guandine–HCl, pH 7.8); Lane 2, pass through; Lanes 3 and 4, binding buffer (8 M urea, pH 7.8); Lanes 5 and 6, wash buffer (8 M urea, pH 6.8); Lanes 7–9, wash buffer (8 M urea, pH 6.8, 10 mM imidazole); Lanes 10–12, elution buffer (8 M urea, pH 4); Lanes 13 and14, elution buffer (8 M urea, pH 3, 300 mM imidazole); and Lanes 15 and 16, elution buffer (8 M urea, pH 3, 500 mM imidazole). (b) The fractions containing target protein (Lanes 7–9, 11 and 12) were pooled (Lane 17), concentrated (Lane 18), and free of urea (Lane 19); and Lane 21 was contents of Lane 20 but free of urea (equal to Lane 10). Both the major band (approximately 55 kDa) and the minor band (approximately 35 kDa) were sequenced through liquid chromatography/mass spectrometry (MS) /MS, provide by a biotechnological company. Based on database searches, those two products were identified as KMO proteins.

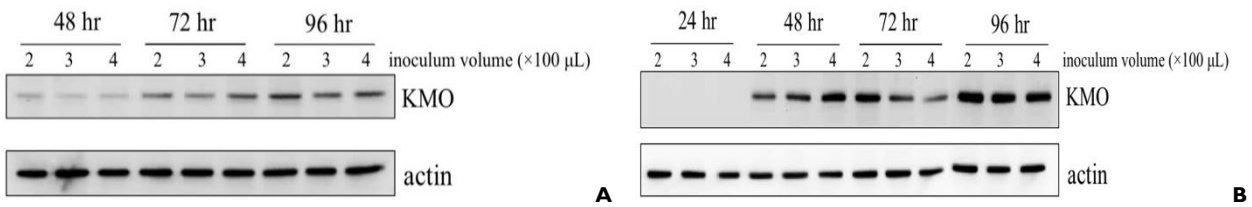

Fig. 3: Optimization of expression condition of cKMO in Sf9 cells. (A) The upper panels showed the Sf9 cell infected with P2 baculovirus; (B) The lower panels showed the cells infected with P3 baculovirus in different inoculum volumes and infection times. The most efficient expression conditions were observed at 72-96 h after infection with 200 µL of P3 virus.

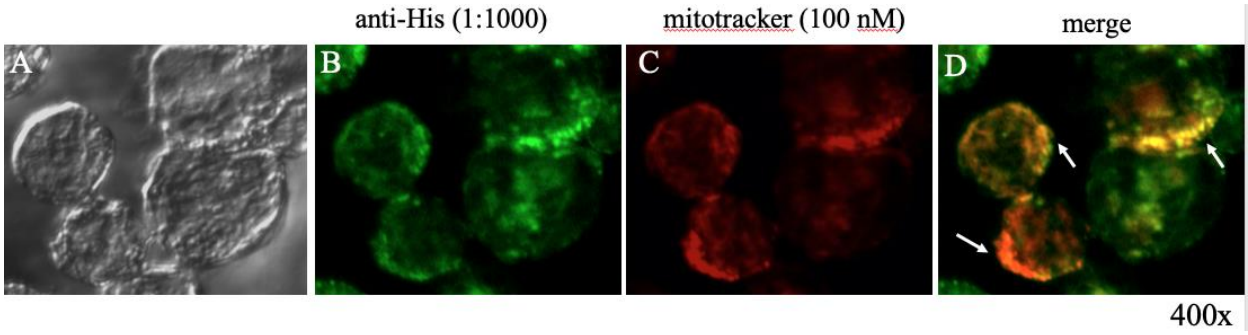

Fig. 4: Subcellular location of recombinant cKMO in Sf9 cells. Sample images of infected Sf9 cells: (A) The same cells were photographed first with transmission light, (B) Fluorescein isothiocyanate-green filter set for fluorescence signal of recombinant His-cKMO (C) MitoTracker red-filter set for MitoTracker staining. (D) Colocalization of His-cKMO protein and mitochondria appear yellow fluorescence in the merged image (arrows).

Table 1: Sequence of oligonucleotide primers and predicted PCR product size of cKMO and GAPDH

Primers	Sequence	Template	Predicted PCR product size
pUC/M13-F pUC/M13-R	5'-CCCAGTCACGACGTTGTAAAACG-3' 5'-AGCGGATAACAATTTCACACAGG-3'	cKMO/Bacmid	3.8 kb
		Bacmid alone	0.3 kb
		Bacmid transposed with pFastBac HT A (without cKMO)	2.4 kb
KMO438-F KMO962-R	5'-CACAGTGGTTGGATCTGACG-3' 5'-AAGCCTGCATTCATTCCTTG-3'	cKMO	0.5 kb
GAPDH-F GAPDH-R	5'-GACGGACCCTCTGGAAAA-3' 5'-ACCAGCTGATGAGCTTGAC-3'	GAPDH of Sf9 cell	0.4 kb

Identifying subcellular location of recombinant cKMO: Moreover, the subcellular location of the expressed cKMO in the Sf9 cells was investigated because the overexpression of membrane proteins often results in protein aggregation. The IFA results revealed that the MitoTracker fluorescence signal and His-tagged recombinant cKMO signal were present at the same location (Fig. 4). These findings indicated that the recombinant cKMO protein was properly folded and correctly transported to the mitochondria in the Sf9 cells.

DISCUSSION

Production of recombinant cKMO protein is a challenging task because of the properties of cKMO. It is a mitochondrial membrane protein, which is expressed in a water-insoluble form or folds incorrectly when expressed (Goffart *et al.*, 2007; Madeo *et al.*, 2009). Three findings indicated that the C-terminal of cKMO may be responsible for mitochondrial anchoring. First, integral membrane proteins can be composed of one or more membrane-spanning domains, which are usually represented by two structural elements, namely hydrophobic α-helices and β-barrels. On average, a length corresponding to at least 21 residues of an α-helical coil are required to approximate the thickness of a phospholipid bilayer (Eisenberg, 1984). According to the amino acid sequence analysis (Fig. 1A), the N-terminal of cKMO is essential for FAD binding where is unlikely to be involved in membrane anchoring (Alberati-Giani *et al.*, 1997). Second, the hydropathy plot, determined by Kyte–Doolittle, identified that the C-terminal of cKMO presents a relatively short hydrophobic region, which may serve as the transmembrane domain (Fig. 1C). Third, additional evidence in support of the hypothesis that residues 432–453 near the C-terminal of swine KMO are essential for mitochondrial targeting is that the deletion of these residues resulted in the mutant enzyme that was mistargeted to the cytosol. Furthermore, the amino acid alignment diagram shows the similar patterns in the C-terminus in the canine and swine KMO (Fig. 1B). The speculative transmembrane domain is flanked on both sides by positively charged residues, which is a critical feature for the insertion to the outer membrane in swine KMO (Hirai *et al.*, 2010).

Several steps for the expression and purification were improved in this study. First, recombinant baculovirus was generated from site-specific transposition propagated in *E. coli*-competent cells. This method reduced the need for plaque purification when a homologous recombination between baculovirus and target DNA occurs in Sf9 cells. Second, the conditions for expression were optimized because the infective ability and duration of baculovirus and Sf9 cell viability are crucial factors. Sf9 cells infected with P3 baculovirus at a MOI of 1.5 for 72-96 h can produce relatively high yields of recombinant cKMO protein. Third, membrane protein purification was performed under denaturing conditions in which the pH and imidazole gradient were changed slightly. The amount of proteins in soluble fraction can be increased using solubilization methods that require a detergent or denaturing agent, such as 5% sodium deoxycholate, 8 M urea, or 6 M guanidine–HCl. The denaturing agent should be used sparingly to ensure concentration of the protein. Moreover, ethanol precipitation, which was used for urea removal, improved the protein yield. All these improvements enabled us to reach higher protein yield of cKMO in baculovirus expression system than has been previously.

This is the first study on the investigation and successful expression of full-length cKMO by using a baculovirus protein expression system. Despite the identification of KMO as a novel target for the treatment of human neurodegenerative disorders, the potential role of KMO in tumorigenesis is incompletely understood. This study provided an efficient method for canine KMO

production that can be utilized for antibody preparation applied in CMT diagnosis. The functions of KMO in canine cancer development should be further investigated in the future.

Authors contribution: CS Lin conceived and supervised the study; CS Lin and CC Liu designed experiments; HY Chen and BH Liu performed experiments and analyzed data; HY Chen and CC Liu wrote the manuscript.

Acknowledgements: This work was supported by Ministry of Science and Technology of Taiwan, Republic of China (NSC 102-2313-B-002-031-MY3).

REFERENCES

Alberati-Giani, Cesura AM, Broger C, *et al.,* 1997. Cloning and functional expression of human kynurenine 3-monooxygenase. FEBS Lett 410:407-12.

Amaral M, Levy C, Heyes DJ, *et al.,* 2013. Structural basis of kynurenine 3-monooxygenase inhibition. Nature 496:382-5.

Breton J, Avanzi N, Magagnin S, *et al.,* 2000. Functional characterization and mechanism of action of recombinant human kynurenine 3-hydroxylase. Eur J Biochem 267:1092-9.

Chiu YH, Lei HJ, Huang KC, *et al.,* 2019. Overexpression of Kynurenine-3-monooxygenase correlates with cancer malignancy and predicts poor prognosis in canine mammary gland tumors. J Oncol 6201764.

Courtney SA, 2010. Modulation of the kynurenine pathway for the potential treatment of neurodegenerative diseases. In: Dominguez C. (Ed.)., Neurodegenerative Diseases. Springer, New York, pp:149-76.

Campbell BM, Charych E, Lee AW *et al.,* 2014. Kynurenines in CNS disease: regulation by inflammatory cytokines. Front Neurosci 8:1-22.

CS H, 2018. Surgery of the reproductive and genital systems. In: Fossum TW (Ed.)., Small Animal Surgery. Mosby Elsevier, Missouri, pp:702-54.

Goffart S, Martinsson P, Malka F, *et al.,* 2007. The mitochondria of cultured mammalian cells: II. Expression and visualization of exogenous proteins in fixed and live cells. Methods Mol Biol 372:17-32.

Hirai K, Kuroyanagi H, Tatebayashi Y, *et al.,* 2010. Dual role of the carboxyl-terminal region of pig liver L-kynurenine 3-monooxygenase: mitochondrial-targeting signal and enzymatic activity. J Biochem 148:639-50.

Jin H, Zhang Y, You H, *et al.,* 2015. Prognostic significance of kynurenine 3-monooxygenase and effects on proliferation, migration, and invasion of human hepatocellular carcinoma. Sci Rep 5:10466.

Moe L, 2001. Population-based incidence of mammary tumours in some dog breeds. J Reprod Fertil Suppl 57:439-43.

Merlo DF, Rossi L, Pellegrino C, *et al.,* 2008. Cancer incidence in pet dogs: findings of the Animal Tumor Registry of Genoa, Italy. J Vet Intern Med 22:976-84.

O'Reilly DR, Miller LK and Luckow VA, 1994. Virus methods, in baculovirus expression vectors: a laboratory manual. Oxford University Press, Inc., New York pp:124-38.

O'Shaughnessy L and Doyle S, 2011. Purification of proteins from baculovirus-infected insect cells. In: Walls LSD (Ed.). Protein Chromatography, Humana Press, New York pp:295-309.

Sahm F, Oezen I, Opitz CA, *et al.,* 2013. The endogenous tryptophan metabolite and NAD+ precursor quinolinic acid confers resistance of gliomas to oxidative stress. Cancer Res 73:3225-34.

Smith JR, Jamie JF and Guillemin GJ, 2016. Kynurenine-3-monooxygenase: a review of structure, mechanism, and inhibitors. Drug Discov Today 21:315-24.

Walczak K, Turski WA and Rzeski W, 2012. Kynurenic acid enhances expression of p21 Waf1/Cip1 in colon cancer HT-29 cells. Pharmacol Rep 64:745-50.

Walczak K, Turski WA and Rajtar G, 2014. Kynurenic acid inhibits colon cancer proliferation in vitro: effects on signaling pathways. Amino Acids 46:2393-401.

Wilson K, Mole DJ, Binnie M, *et al.,* 2014. Bacterial expression of human kynurenine 3-monooxygenase: solubility, activity, purification. Protein Expr Purif 95:96-103.